JACS
JOURNAL OF THE AMERICAN CHEMICAL SOCIETY

Communication

pubs.acs.org/JACS

Inosine Nucleobase Acts as Guanine in Interactions with Protein Side Chains

Matea Hajnic, Anita de Ruiter,[†] Anton A. Polyansky, and Bojan Zagrovic*

Department of Structural and Computational Biology, Max F. Perutz Laboratories, University of Vienna, Campus Vienna Biocenter 5, Vienna A-1030, Austria

Supporting Information

ABSTRACT: A central intermediate in purine catabolism, the inosine nucleobase hypoxanthine is also one of the most abundant modified nucleobases in RNA and plays key roles in the regulation of gene expression and determination of cell fate. It is known that hypoxanthine acts as guanine when interacting with other nucleobases and base pairs most favorably with cytosine. However, its preferences when it comes to interactions with amino acids remain unknown. Here we present for the first time the absolute binding free energies and the associated interaction modes between hypoxanthine and all standard, non-glycyl/non-prolyl amino acid side chain analogs as derived from molecular dynamics simulations and umbrella sampling in high- and low-dielectric environments. We illustrate the biological relevance of the derived affinities by providing a quantitative explanation for the specificity of hypoxanthine-guanine phosphoribosyltransferase, a key enzyme in the purine salvage pathway. Our results demonstrate that in its affinities for protein side chains, hypoxanthine closely matches guanine, much more so than its precursor adenine.

Inosine nucleobase hypoxanthine (HPA) is present in the cell either in a monomeric form or within nucleic acids where it is predominantly introduced by adenine deamination at the C6 position[1,2] (Figure 1A). Monomeric HPA is an intermediate in purine catabolism but is also used as a nitrogen source in bacterial and parasite cultures.[3,4] Generally seen as damage in the case of DNA, HPA in RNA is an essential modification introduced by specific deaminases.[2] Notably, HPA preferentially base pairs with cytosine (CYT), making it more similar to guanine (GUA) than to its precursor adenine (ADE) when it comes to interactions with other nucleobases (Figure 1A). With a recently estimated count of several million sites where ADE can get deaminated in human RNA alone,[5] HPA is one of the most abundant modified nucleobases in biological systems and has been identified in mRNAs, tRNAs, snoRNAs, miRNAs, and lincRNAs.[1] Moreover, the frequency of ADE deamination increases even further in tumor cells.[6] As a part of RNA, HPA plays important roles in the regulation of immune response,[7] control of gene expression, and determination of cell fate by, for example, introducing new mRNA splice sites,[8] affecting transcript localization[9] and stability,[10] or enabling protein recoding.[11] Importantly, these processes often depend on RNA/protein interactions in which HPA contributes directly to binding.[12−14] This is in part due to the fact that ADE deamination destabilizes double-stranded regions in nucleic acids[15] and thus increases the accessibility of nucleobases to protein residues. However, despite the ubiquity and biological significance of such interactions, their physicochemical foundation remains unexplored. This, in particular, concerns the interaction preferences between HPA and amino acid side chains at RNA/protein interfaces and the associated binding mechanisms.

We present here a systematic study of hypoxanthine binding to all standard non-glycyl/non-prolyl amino acid side chain analogs using molecular dynamics (MD) simulations and umbrella sampling (US) (details in SI). Our study is, to the best of our knowledge, the first to examine hypoxanthine interaction propensities with amino acid side chains. In particular, we compare the obtained affinities to those of non-modified nucleobases, derived using the same methodology.[16] Our simulations are run in both water and methanol, whereby the latter is used to mimic a low-dielectric environment at the typical RNA/protein interfaces.[17,18] Importantly, the GROMOS 54A8 parameter set, used herein, has been optimized to capture accurately amino acid hydrophobicity,[19,20] a key factor in nucleobase/amino acid interactions. In addition, we have previously shown that the GUA/amino acid side chain absolute binding free energies, calculated using GROMOS 54A8,[19] closely match the only extensive, analogous experimental set available, that of association free energies between guanosine and eight different amino acids (Pearson R^2 = 0.76).[16] Further validation in this context was recently provided by comparing against experiment the simulation-derived interaction free energies between all 20 standard amino acids and a nucleobase mimetic 2,6-dimethylpyridine (Pearson R^2 = 0.74).[21]

Potential of mean force (PMF) curves calculated from simulations in water show that HPA has a preference for aromatic side chains (Figure 1B, upper panel) with the corresponding binding free energies ranging from −4.9 kJ/mol for Trp to −3.1 kJ/mol for Phe (Figure 1C, ΔG_{wHPA}). Favorable, albeit weaker, binding is also observed in the case of other non-polar side chains (Figures 1C and S1A). On the other hand, affinities of HPA for polar or charged side chains in water are mostly negligible or unfavorable (Figure 1B lower panel, Figure 1C, ΔG_{wHPA}, Figure S1A). Interestingly, the same trend was observed in a related study where all five standard, non-modified RNA/DNA nucleobases showed the highest

Received: March 10, 2016
Published: April 19, 2016

DOI: 10.1021/jacs.6b02417
J. Am. Chem. Soc. 2016, 138, 5519−5522

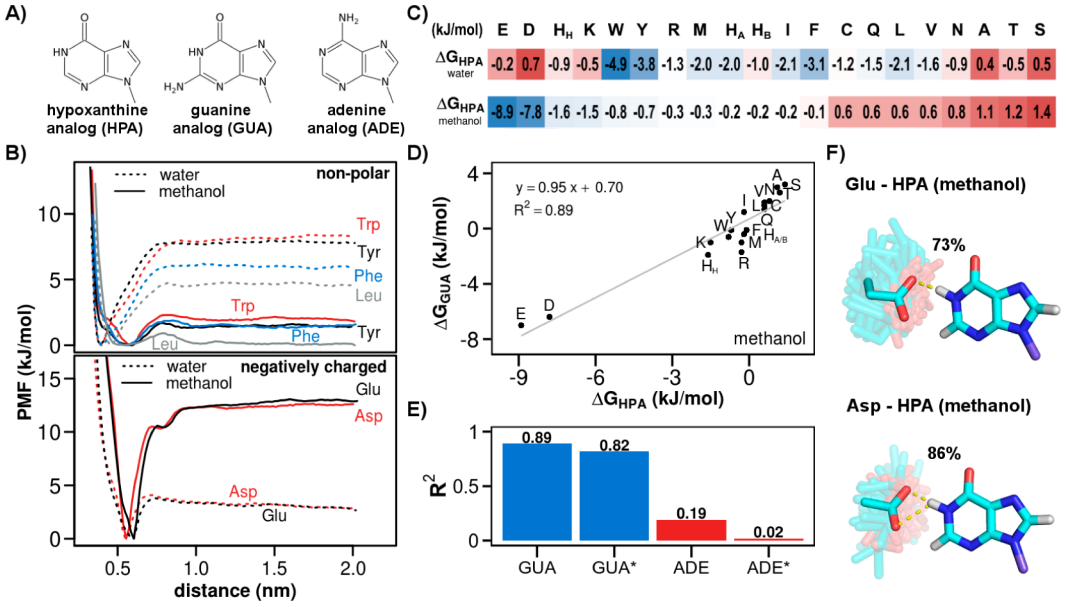

Figure 1. (A) Chemical structures of HPA, GUA, and ADE methylated at N9 position. (B) PMF curves derived for amino acid side chains whose affinities for HPA change significantly (more than 1 k_BT, T = 298 K) depending on the surrounding solvent. For side chains in the upper panel, affinities for HPA are less favorable with a decrease in the dielectric constant of the solvent, while for those in the lower panel, the opposite is observed. (C) Binding free energies between HPA and side chains in water and methanol. (D) Correlation between HPA and GUA[16] side chain affinities in methanol. (E) R^2 coefficients between HPA and GUA[16] or HPA and ADE[16] side chain affinities in methanol. (*) denotes R^2 coefficients with values for Glu and Asp excluded. (F) Members of the most dominant clusters at the optimal binding distance for Glu and Asp (r_0 = 6 Å) with HPA in methanol, together with the associated occupancies. Cluster centers are shown in the foreground.

preference for aromatic side chains and the weakest for charged ones in water.[16] In fact, HPA binding free energies in water correlate closely with those of non-modified nucleobases derived in that study[16] with all Pearson R^2 coefficients higher than or equal to 0.77, e.g. $R^2_{\text{HPA-GUA}}$ = 0.94 and $R^2_{\text{HPA-ADE}}$ = 0.81 (Table S1A). Moreover, the values of root-mean-squared deviation (RMSD) between HPA and the non-modified nucleobase affinity scales are all below 1.31 kJ/mol (the lowest with GUA affinities of 0.52 kJ/mol), another indication that the scales do not differ significantly from each other (Table S2A).

On the other hand, PMF curves derived from simulations in the low-dielectric methanol show significantly different trends (Figure S1B). The most evident difference concerns the negatively charged side chains (Figure 1B, lower panel). While in water, HPA has no preference for Glu and Asp, it exhibits the highest affinity for these side chains in methanol, with binding free energies of −8.9 and −7.8 kJ/mol, respectively (Figure 1B,C). Another prominent difference is that HPA exhibits negligible preference for aromatic side chains in methanol (Figure 1B,C). In addition, we observe a significant change in HPA affinity ($\Delta\Delta G > 1\ k_BT$) for Leu as well (Figure 1B,C). HPA affinities do not change drastically for other side chains, although most of the preferences do get weaker (Figures 1C and S1). When comparing HPA affinities for side chains with those of non-modified nucleobases derived in methanol,[16] the strongest correlation is obtained for GUA (R^2 = 0.89, Figure 1D). Both HPA and GUA show the strongest affinity for Glu and Asp, but the general trends in their affinities remain matched even if these two amino acids are excluded (R^2 = 0.82, Figure 1E). On the other hand, R^2 between HPA and ADE affinities derived in methanol equals 0.19 (or 0.02 without Glu and Asp, Figures 1E and S2, Table S1B). Moreover, the RMSD between the HPA and GUA scales is the lowest ($\text{RMSD}_{\text{HPA-GUA}}$ = 1.14 kJ/mol) when compared to those of other non-modified nucleobases including ADE[16] (e.g., $\text{RMSD}_{\text{HPA-ADE}}$ = 3.57 kJ/mol, Table S2B). The main difference between HPA and ADE affinities can be ascribed to the charged Glu, Asp, Lys, and Arg that do not bind favorably to ADE in methanol, but marked deviation is seen for other side chains as well (Figure S2). Thus, HPA affinities for side chains in methanol are most similar to those of GUA, and not those of its precursor ADE.

The observed change in HPA affinities for protein side chains in water and methanol is a consequence of two principal factors: (i) the destabilization of stacking interactions in the low-dielectric environment, and (ii) the significant screening of electrostatic interactions in bulk water. In the case of both GUA and HPA, it is precisely the electrostatic interactions that are responsible for the strongest binding free energies of Glu and Asp with these bases in methanol. In particular, while the carboxyl oxygen atoms of Glu and Asp form bidentate hydrogen bonds with N1 and the amino group at C2 in the Watson−Crick edge of GUA,[16] they prefer to form a bifurcated hydrogen bond with the N1 of HPA (Figure 1F). It is interesting that despite the presence of an additional hydrogen bond donor in GUA, i.e., the amino group at C2, its binding free energies and the dominant binding geometries with the acidic side chains are very similar to those of HPA (Figure 1F).

We illustrate the biological relevance of the obtained HPA affinities for side chains in the case of hypoxanthine-guanine phosphoribosyltransferase (HGPRT), a metabolic enzyme that specifically recognizes and binds HPA and GUA.[22] HGPRT catalyzes the conversion of HPA and GUA to their nucleotide forms as a part of the purine salvage pathway by attaching the 5-phosphoribosyl group from 5-phosphoribosyl-1-pyrophosphate to the N9 position of the two nucleobases. The specificity of the enzyme critically depends on Lys 165 in the binding pocket of the active site[23] whose amino group can form a hydrogen bond with the exocyclic oxygen at C6 of HPA and

DOI: 10.1021/jacs.6b02417
J. Am. Chem. Soc. 2016, 138, 5519−5522

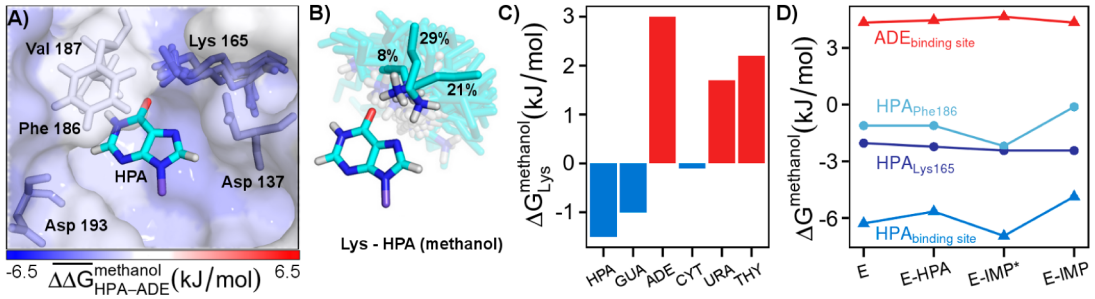

Figure 2. (A) X-ray structure of the HGPRT nucleobase binding site (PDB ID: 1HMP) with HPA modeled in. Lys 165 is the key specificity determinant in binding. The binding site is colored according to the spatially averaged difference between side chain binding free energies for HPA and ADE in methanol derived in this study. The ensemble of Lys 165 conformations was derived from crystal structures of HGPRT enzyme in different stages of the catalytic cycle (PDB IDs: 1Z7G, ID6N, 1BZY, 1HMP). (B) Centers of the three most dominant clusters at the optimal binding distance (r_0 = 6 Å) between HPA and Lys in our simulations, accounting for a total of 58% of all conformers at that distance. (C) Binding-free energies derived in methanol between Lys and HPA/nonmodified nucelobases.[16] (D) Spatially averaged affinities of the nucleobase binding site of HGPRT enzyme for HPA and ADE at different catalytic stages (E, APO enzyme; E-HPA, enzyme with substrate bound; E-IMP*, enzyme with reaction transition state; E-IMP, enzyme with product bound) based on the crystal structures (PDB IDs: 1Z7G, ID6N, 1BZY, 1HMP, respectively), with the contributions of Lys 165 and Phe 186 also shown.

GUA (Figures 1A and 2A), a position where ADE has an amino group[23] (Figure 1A). Using the values obtained for side chains in methanol, we have mapped the differences between HPA and ADE affinities onto the surface of the HGPRT crystal structure with HPA modeled in the binding site (Figure 2A). Indeed, the protein region around the substrate's exocyclic oxygen (Lys 165, Asp 137) shows favorable affinities for HPA with respect to ADE (Figure 2A). Interestingly, when we cluster conformations of the HPA/Lys pair from our methanol MD simulations at the distance with the most favorable binding free energy and no conformational restraints applied, we get predominantly the same conformation between the two monomers (total occupancy of 58%) as observed in the experimental HGPRT structures (Figure 2A,B). Furthermore, by just comparing the binding free energies between Lys and HPA and all nonmodified nucleobases derived in methanol,[16] it is clear that Lys interacts favorably with HPA and GUA and least favorably with ADE, with differences between Lys affinities to HPA/GUA and ADE being 4.5 and 4 kJ/mol, respectively (Figure 2C). In addition, interactions between Lys and other standard nucleobases are free energetically either unfavorable (URA and THY) or negligible (CYT). Finally, we have also compared how the spatially averaged affinity for HPA and ADE of the residues in the HGPRT nucleobase-binding site changes during different catalytic stages (Figure 2D). While HGPRT shows no favorable affinity for ADE, the opposite is true for HPA. Interestingly, Lys 165 changes neither its conformation (Figure 2A) nor local affinity in different states of the enzyme (Figure 2D). On the other hand, the average local affinity for HPA changes the most at Phe 186, which is also responsible for changes in the overall affinity of the nucleobase-binding site (Figure 2D) and agrees with an experimental finding that Phe 186 stabilizes the nucleobase in the transition state.[24] Finally, our affinities support the idea that the promiscuity of *Plasmodium* HGPRT relative to human may partly be due to the difference in tightness of the bound nucleobase in the transition state (details in SI). Therefore, the low-dielectric affinity scales derived herein provide a direct, quantitative explanation for the ability of HGPRT to discriminate between HPA/GUA and ADE.

In summary, we have for the first time given evidence that HPA mimics GUA in its interactions with standard protein side chains, paralleling its known behavior in interactions with other nucleobases. Importantly, HPA's quantitative mimicry of GUA regarding nucleobase/side chain affinities and geometries extends to both high- and low-dielectric environments. The latter is particularly relevant considering the largely dehydrated, low-dielectric nucleic acid/protein interfaces.[17,18] In addition to HGPRT, this finding provides explanation for the behavior of several other systems, including *E. coli* membrane transporters YjcD and YgfQ[25] specific only for HPA and GUA and HIV *rev*[26] and *tat*[27] proteins that do not distinguish between the two. Finally, it has been shown that HPA-rich transcripts regulate gene expression by either being recognized and kept within the nucleus by specialized multiprotein complexes[12,13] or degraded by specific endonucleases.[14] With the rising importance of HPA as a source of epigenetic diversity in RNA, it is our hope that its binding affinities for protein side chains will help understand better not only these systems but also those yet to emerge. Our results, in particular, support a mechanism in which this modification acts by switching the ADE interaction modes with both nucleic acids and proteins to those of GUA.

■ ASSOCIATED CONTENT

Supporting Information

The Supporting Information is available free of charge on the ACS Publications website at DOI: 10.1021/jacs.6b02417.

Experimental details and data (PDF)

■ AUTHOR INFORMATION

Corresponding Author

*bojan.zagrovic@univie.ac.at

Present Address

†BOKU, Muthgasse 18, Vienna, A-1190, Austria

Notes

The authors declare no competing financial interest.

■ ACKNOWLEDGMENTS

The authors gratefully acknowledge Prof. C. Oostenbrink for help with parametrization of hypoxanthine. This work was supported by European Research Council grant 279408 to B.Z.

■ REFERENCES

(1) Nishikura, K. *Nat. Rev. Mol. Cell Biol.* **2016**, *17*, 83.

DOI: 10.1021/jacs.6b02417
J. Am. Chem. Soc. 2016, 138, 5519−5522

(2) Alseth, I.; Dalhus, B.; Bjørås, M. *Curr. Opin. Genet. Dev.* **2014**, *26*, 116.
(3) Berman, P. A.; Human, L.; Freese, J. A. *J. Clin. Invest.* **1991**, *88*, 1848.
(4) De la Riva, L.; Badia, J.; Aguilar, J.; Bender, R. A.; Baldoma, L. *J. Bacteriol.* **2008**, *190*, 7892.
(5) Bazak, L.; Haviv, A.; Barak, M.; Jacob-Hirsch, J.; Deng, P.; Zhang, R.; Isaacs, F. J.; Rechavi, G.; Li, J. B.; Eisenberg, E.; Levanon, E. Y. *Genome Res.* **2014**, *24*, 365.
(6) Fumagalli, D.; Gacquer, D.; Rothé, F.; Lefort, A.; Libert, F.; Brown, D.; Kheddoumi, N.; Shlien, A.; Konopka, T.; Salgado, R.; Larsimont, D.; Polyak, K.; Willard-Gallo, K.; Desmedt, C.; Piccart, M.; Abramowicz, M.; Campbell, P. J.; Sotiriou, C.; Detours, V. *Cell Rep.* **2015**, *13*, 277.
(7) Liddicoat, B. J.; Piskol, R.; Chalk, A. M.; Ramaswami, G.; Higuchi, M.; Hartner, J. C.; Li, J. B.; Seeburg, P. H.; Walkley, C. R. *Science* **2015**, *349*, 1115.
(8) Rueter, S. M.; Dawson, T. R.; Emeson, R. B. *Nature* **1999**, *399*, 75.
(9) Prasanth, K. V.; Prasanth, S. G.; Xuan, Z.; Hearn, S.; Freier, S. M.; Bennett, C. F.; Zhang, M. Q.; Spector, D. L. *Cell* **2005**, *123*, 249.
(10) Wang, I. X.; So, E.; Devlin, J. L.; Zhao, Y.; Wu, M.; Cheung, V. G. *Cell Rep.* **2013**, *5*, 849.
(11) Higuchi, M.; Single, F. N.; Köhler, M.; Sommer, B.; Sprengel, R.; Seeburg, P. H. *Cell* **1993**, *75*, 1361.
(12) Zhang, Z.; Carmichael, G. G. *Cell* **2001**, *106*, 465.
(13) Wang, Q.; Zhang, Z.; Blackwell, K.; Carmichael, G. G. *Curr. Biol.* **2005**, *15*, 384.
(14) Morita, Y.; Shibutani, T.; Nakanishi, N.; Nishikura, K.; Iwai, S.; Kuraoka, I. *Nat. Commun.* **2013**, *4*, 2273.
(15) Bass, B. L.; Weintraub, H. *Cell* **1988**, *55*, 1089.
(16) de Ruiter, A.; Zagrovic, B. *Nucleic Acids Res.* **2015**, *43*, 708.
(17) Nott, T. J.; Petsalaki, E.; Farber, P.; Jervis, D.; Fussner, E.; Plochowietz, A.; Craggs, T. D.; Bazett-Jones, D. P.; Pawson, T.; Forman-Kay, J. D.; Baldwin, A. J. *Mol. Cell* **2015**, *57*, 936.
(18) Li, L.; Li, C.; Zhang, Z.; Alexov, E. *J. Chem. Theory Comput.* **2013**, *9*, 2126.
(19) Schmid, N.; Eichenberger, A. P.; Choutko, A.; Riniker, S.; Winger, M.; Mark, A. E.; van Gunsteren, W. F. *Eur. Biophys. J.* **2011**, *40*, 843.
(20) Reif, M. M.; Hünenberger, P. H.; Oostenbrink, C. *J. Chem. Theory Comput.* **2012**, *8*, 3705.
(21) Hajnic, M.; Osorio, J. I.; Zagrovic, B. *Phys. Chem. Chem. Phys.* **2015**, *17*, 21414.
(22) Krenitsky, T. A.; Papaioannou, R.; Elion, G. B. *J. Biol. Chem.* **1969**, *244*, 1263.
(23) Eads, J. C.; Scapin, G.; Xu, Y.; Grubmeyer, C.; Sacchettini, J. C. *Cell* **1994**, *78*, 325.
(24) Karnawat, V.; Gogia, S.; Balaram, H.; Puranik, M. *ChemPhysChem* **2015**, *16*, 2172.
(25) Papakostas, K.; Botou, M.; Frillingos, S. *J. Biol. Chem.* **2013**, *288*, 36827.
(26) Iwai, S.; Pritchard, C.; Mann, D. A.; Karn, J.; Gait, M. J. *Nucleic Acids Res.* **1992**, *20*, 6465.
(27) Hamy, F.; Asseline, U.; Grasby, J.; Iwai, S.; Pritchard, C.; Slim, G.; Butler, P. J.; Karn, J.; Gait, M. J. *J. Mol. Biol.* **1993**, *230*, 111.

DOI: 10.1021/jacs.6b02417
J. Am. Chem. Soc. 2016, 138, 5519−5522